

# Natural Radioactivity Measurements of Basalt Rocks in Sidakan District Northeastern of Kurdistan Region-Iraq

Ali A. Ahmed<sup>1</sup>, Mohammed I. Hussein<sup>2</sup>

**Abstract**—The amounts of radioactivity in the igneous rocks have been investigated; samples were collected from the total of eight basalt rock types in the northeastern of Kurdistan region/Iraq. The activity concentration of <sup>226</sup>Ra (<sup>238</sup>U) series, <sup>228</sup>Ac (<sup>232</sup>Th) series, <sup>40</sup>K and <sup>137</sup>Cs were measured using Planar HPGe and NaI(Tl) detectors. Along the study area the radium equivalent activities  $R_{eq}$  in Bq/Kg of samples under investigation were found in the range of 22.16 to 77.31 Bq/Kg with an average value of 44.8 Bq/Kg, this value is much below the internationally accepted value of 370 Bq/Kg. To estimate the health effects of this natural radioactive composition, the average values of absorbed gamma dose rate  $D$  (55 nGy<sup>h</sup><sup>-1</sup>), Indoor and outdoor annual effective dose rates  $E_{ied}$  (0.11 mSv<sup>y</sup><sup>-1</sup>) and  $E_{oed}$  (0.03 mSv<sup>y</sup><sup>-1</sup>), External hazard index  $H_{ex}$  (0.138) and internal hazard index  $H_{in}$  (0.154), and representative level index  $I_{\gamma}$  (0.386) have been calculated and found to be lower than the worldwide average values.

**Keywords**—Absorbed dose, activity concentration, igneous rocks, HPGe, NaI(Tl), Natural Radioactivity.

## I. INTRODUCTION

OUR world is radioactive and has been since it was created. Over 60 radionuclides can be found in nature. Radionuclides are found in air, water and soil, and additionally in us, being that we are products of our environment. Every day, we ingest/inhale nuclides in the air we breathe, in the food we eat and the water we drink. Radioactivity is common in the rocks and soil that makes up our planet, in the water and oceans, and even in our building materials and homes. It is just everywhere. There is no where on Earth that you can get away from Natural Radioactivity [1 and 2].

Distribution of naturally occurring radionuclides mainly <sup>238</sup>U, <sup>232</sup>Th and <sup>40</sup>K and other radioactive elements depends on the distribution of rocks from which they originate and on the processes through which they are concentrated [3]. The main sources of the external  $\gamma$ -radiation are the radionuclides of the U and Th series and <sup>40</sup>K [4]. Radium and its ultimate precursor uranium in the ground are the source of radon an  $\alpha$ -radioactive inert gas. As an inert gas and having sufficiently long lifetime (3.8 days) it can move freely through the materials like soil, sand, rock etc. Short lived radon progenies have been established as causative agents of lung cancer [3]. Radon appears when radium (<sup>226</sup>Ra) – <sup>238</sup>U-family division product – splits up.

In many countries the most important source of radon is the ground, however, it is possible that radon's volumetric activity indoors is determined by building materials, water-supply [5]. Therefore the assessment of gamma radiation dose from natural sources is of particular importance as natural radiation is the largest contributor to the external dose of the world population [2]. Cesium-137 is one of the most important contaminants from fallout nuclear debris because of its long physical half-life and affinity for biological systems. Body burdens of this radionuclide in man result principally from the food-chain sequence: air and precipitation to plants, plants to milk and meat, with dairy and beef cattle as the principal vectors between plants and man's diet. This apparently simple relation describes the food-chain pattern for cesium 137 quite adequately since uptakes of cesium 137 by plants from soil are negligible [6].

Due to the unusual circumstances of Kurdistan and Iraq during the last three decades, a limited number of studies exist concerning this important field of investigation. For this the present study has been proposed to cover and establish a base line data for the regional radioactivity.

The studied area is located in the northeastern of Kurdistan region, Iraq, in the Erbil Governorate, Soran town Sidakan district, Fig. 1;



Fig. 1 Location map of the studied area in the northeastern part of Kurdistan region, Erbil, Iraq [7].

<sup>1</sup> Iraq/Kurdistan Region/ University of Salahaldeen, College of Science, Physics Dept. (e-mail:aha66sara@yahoo.com)

<sup>2</sup> Iraq/Kurdistan Region/ University of Salahaldeen, College of Science, Physics Dept. (m\_issa76@yahoo.com)

The studied area contains volcanic igneous rocks which are belongs to Walsh volcanic Group. The age of Walsh group is probably Paleocene-Eocene and may extend into Oligocene. The samples had been collected in Bardbizin Mountain, Kanishilana and Rubarok area around the Sidakan district in the northeastern of Kurdistan region, which lies within the Zagros thrust Belt. It is formed during middle Alpine Orogeny. The collected samples are igneous rocks of extrusive and Basalt types and composed of the major minerals (Pyroxene, Calcium-rich Plagioclase Feldspars and Olivine). The location of the studied area has been determined using the Global Positioning System (GPS):

Latitude: 36°49'45.4"N.  
 Longitude: 44°47'37.9"E.

## II. EXPERIMENTAL METHODS

### A. Samples collection and preparation

Table I illustrates the place and location of each of the 8 collected samples. All samples are taken under the supervision of geological expert in October 2009 from the areas of study and brought to the Laboratory. Basalt rocks were dried and mechanically crushed and grounded by using Grinding Machine to powder it, then equal weights [500 gm and 250 gm for NaI(Tl) and HPGe detectors respectively] of the samples were packed in plastic bags (Marinelli beaker) and sealed for about 4 weeks to reach secular equilibrium between radium and thorium and their progenies. After powdering, the samples were mounted on the detector for counting [21600 seconds and 345600 seconds for NaI(Tl) and HPGe detectors, respectively].

TABLE I  
 SAMPLE LOCATIONS

Samples Code	Location
S1	Kanishilana
S2	Rubarok
S3	Bardbizin
S4	Kanishilana
S5	Rubarok
S6	Rubarok
S7	Kanishilana
S8	Bardbizin

### B. NaI(Tl) Gamma Ray Spectroscopy

The Physical layout of the NaI(Tl) gamma ray spectroscopy are shown in Fig.2. The NaI(Tl) Scintillation detector has an active area of 2×2 inches, energy resolution 11.3% and Efficiency of 1.2 % at the 662keV Cs-137 line , the detector is of Saint-Gobain type 38 S 51, Photomultiplier PM type 9266 B.

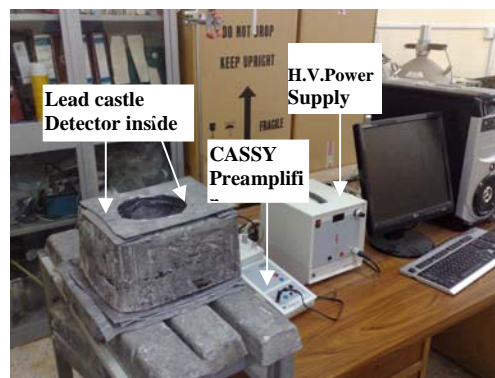


Fig. 2 Physical layout of the NaI(Tl) gamma ray spectroscopy

The lead castle used in this study to Shield the detector had a 10 cm thick. It makes a good shielding material due to its high density and large atomic number. The preamplifier and amplifier of 524 058 CASSY Model, and of 524 010 CASSY Model, respectively, have been used in this work.

### C. HPGe Gamma Ray Spectroscopy

The Physical layout of the HPGe gamma ray spectroscopy is shown in Fig.3.

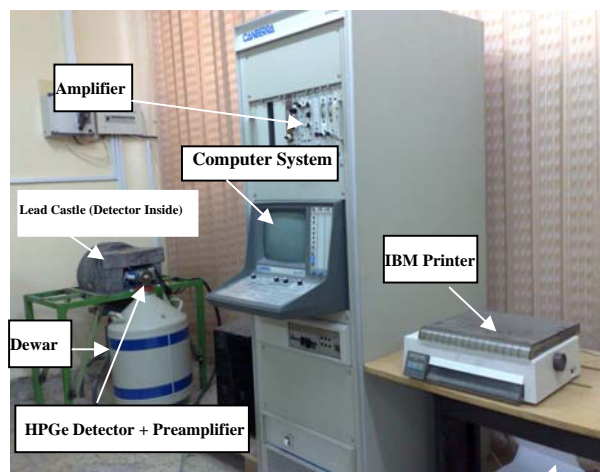


Fig. 3 The physical layout of the HPGe gamma ray spectroscopy.

The detector was the Planar high purity germanium (HPGe) detector of Model PSP10010, serial number 689787, bias Voltage (-500) V with an energy resolution of 0.520 keV at the 122 keV <sup>57</sup>Co line and has the following specifications: Active area 100mm<sup>2</sup>, Active diameter 11.3mm, window thickness 0.075mm, and the Cryostat Model 7600 [8], and has the Efficiency 0.648 % of <sup>226</sup>Ra. The preamplifier and amplifier of Models 2008 CANBERRA, 2020 CANBERRA, respectively, have been used in this work.

## II. DATA ANALYSIS

### A. Sample Spectra and Radionuclide's Identification

The gamma-ray spectrum of each studied sample were taken by both of the NaI(Tl) and Planar HPGe detectors. The

spectroscopy used for detection coupled to Multichannel Analyzer (MCA) [512 and 4096 channels for NaI(Tl) and HPGe detectors respectively]. In the case of NaI(Tl) detector, the spectrum is ranged from (85-1816) keV as shown in Fig. 4. For the case of Planar HPGe detector the spectrum is divided into five energy ranges (9.5-50), (50-100), (100-145), (145-186) and (186-400) keV as shown in Figs. 5, 6, 7, 8, and 9, respectively.

### B. Activity Concentration

Through calculating the area under the peak (net area) and by means of the detector efficiency curve, the specific activity (activity concentration)  $A_z$  was determined using the formula [9].

$$A_s(Bq.Kg^{-1}) = \frac{A}{W} \quad (1)$$

where  $A$  is the activity of the isotope and  $W$  is the Weight of the sample. The expression for the calculation of activity of each isotope was given by [10].

$$A(Bq) = \frac{A_{net}}{\epsilon \times I_\gamma \times t} \quad (2)$$

where  $A_{net}$  is the net area of the total absorption line,  $I_\gamma$  the absolute intensity of the transition,  $t$  the sample counting time, and  $\epsilon$  the gamma efficiency evaluated in function of the transition energy.

### C. Radiation hazard indices

To represent the activity levels of  $^{226}\text{Ra}$ ,  $^{232}\text{Th}$  and  $^{40}\text{K}$  by a single quantity, which takes into account the radiation hazards associated with them, a common radiological index has been introduced. This index is called radium equivalent ( $Ra_{eq}$ ) activity and is mathematically defined by [11]:

$$Ra_{eq}(Bq.Kg^{-1}) = A_{Ra} + 1.43A_{Th} + 0.077A_K \quad (3)$$

where  $A_{Ra}$ ,  $A_{Th}$  and  $A_K$ , are the activity concentrations of  $^{226}\text{Ra}$ ,  $^{232}\text{Th}$  and  $^{40}\text{K}$  respectively. In the above relation, it has been assumed that 10 Bq/Kg of  $^{226}\text{Ra}$ , 7 Bq/Kg of  $^{232}\text{Th}$  and 130 Bq/Kg of  $^{40}\text{K}$  produced equal gamma dose. The absorbed dose rates ( $D$ ) due to gamma radiations in air at 1m above the ground surface for the uniform distribution of the naturally occurring radionuclides ( $^{226}\text{Ra}$ ,  $^{232}\text{Th}$  and  $^{40}\text{K}$ ) were calculated based on guidelines provided by UNSCEAR 2000 [11]. We assumed that the contributions from other naturally occurring radionuclides were insignificant. Therefore,  $D$  can be calculated according to [11]:

$$D(nGy.h^{-1}) = 0.462A_{Ra} + 0.621A_{Th} + 0.0417A_K \quad (4)$$

A widely used hazard index (reflecting the external exposure) called the external hazard index  $H_{ex}$  is defined as follows [11]:

$$H_{ex} = \frac{A_{Ra}}{370} + \frac{A_{Th}}{259} + \frac{A_K}{4810} \quad (5)$$

In addition to external hazard index, radon and its short-lived products are also hazardous to the respiratory organs. The internal exposure to radon and its daughter product is quantified by the internal hazard index  $H_{in}$ , which is given by [11]:

$$H_{in} = \frac{A_{Ra}}{185} + \frac{A_{Th}}{259} + \frac{A_K}{4810} \quad (6)$$

The values of the indices ( $H_{ex}, H_{in}$ ) must be less than unity ( $\leq 1$ ) for the radiation hazard to be negligible [11]. To estimate the annual effective dose rates, the conversion coefficient from absorbed dose (D) in air to effective dose,  $0.7\text{SvGy}^{-1}$  was used for the conversion coefficient from absorbed dose in air to effective dose received by adults, and 0.8 for the indoor occupancy factor and implying that 20% of time is spent outdoors, outdoor occupancy factor of 0.2 proposed by UNSCEAR 2000 were used. The effective dose rate ( $E$ ) in units of  $m\text{Svyr}^{-1}$  was calculated by the following formulae [3]:

Indoor effective dose:

$$E_{ied}(m\text{Svyr}^{-1}) = D(n\text{Gyh}^{-1}) \times 8760h \times 0.8 \times 0.7\text{SvGy}^{-1} \times 10^{-6} \quad (7)$$

Outdoor effective dose:

$$E_{oed}(m\text{Svyr}^{-1}) = D(n\text{Gyh}^{-1}) \times 8760h \times 0.2 \times 0.7\text{SvGy}^{-1} \times 10^{-6} \quad (8)$$

The representative level index,  $I_{\gamma r}$ , used to estimate the level of  $\gamma$ -radiation hazard associated with the natural radionuclides in specific investigated samples, is defined from the following Equation [12]:

$$I_{\gamma r} = \frac{A_{Ra}}{150} + \frac{A_{Th}}{100} + \frac{A_K}{1500} \quad (9)$$

## III. RESULTS AND DISCUSSION

### A. Spectrum Measurements and Radionuclide's Identification

The gamma ray spectrum of each studied sample was taken by both the planar HPGe and NaI(Tl) detectors. The spectroscopy used for detection coupled to Multi Channel Analyzer MCA (4096 and 512 channels for HPGe and NaI(Tl) detectors, respectively). The net sample spectra were obtained by subtracting the background spectrum from (sample + background) spectra as shown in Figs.(4) through (9). The spectrum of sample (4) has been shown for both of the NaI(Tl) and HPGe detectors due to its highest radioactivity among all the studied samples. For the NaI(Tl) detector the collected spectra covers the energy range of 85 to 1816 KeV as shown in Fig. (4). In the case of Planar HPGe detector, the obtained spectra covers the energy range of 9.5 to 400 keV: Figs. (5) to (9) presents the spectrum of sample 4 divided into five energy ranges (9.5-50), (50-100), (100-145), (145-186) and (186-400) keV, respectively. The resulted spectra of all the samples were investigated to identify the radionuclides existence through their  $\gamma$ -ray or x-ray lines. Throughout the spectra and as it is shown in Fig. (4) through (9), the identified intense lines are labeled within the spectra: (Th-234, Pa-234, Ra-226, Pb-214, Bi-214, Pb-210 and Tl-210) belonging to U-238 series, (Ac-228, Th-228, Pb-212 and Bi-212) belonging to Th-232 series,

while Cs-137 and K-40 are not belongs to the above series. For the ascription of  $\gamma$ -ray or X-ray lines Table of isotopes [13], [14], [15], and [16] and nuclear data sheets [17] and [18] have been depended.

*B. Primordial Radionuclides Activity Concentration*

The Activity concentrations in (Bq.Kg<sup>-1</sup>) for the eight studied samples calculated for each of the <sup>238</sup>U (<sup>226</sup>Ra), <sup>232</sup>Th(<sup>228</sup>Ac) and <sup>40</sup>K radionuclides by using equs. (1) and (2), the results are listed in Table II and shown in Figs. (10) and (11) respectively. The data presented in Table II show that radioactive equilibrium between progenies in <sup>238</sup>U and <sup>232</sup>Th series for all samples can be assumed. Measured rock samples are characterized by values of activity concentrations of <sup>228</sup>Ac (<sup>232</sup>Th), <sup>226</sup>Ra (<sup>238</sup>U) and by high radioactivity of <sup>40</sup>K. Calculations of count rates for each

detected photopeaks and activity concentration of detected radionuclides depend on the establishment of secular equilibrium in the samples. Since secular equilibrium was reached between <sup>232</sup>Th and <sup>238</sup>U and their decay products, the <sup>232</sup>Th concentration was determined from the average concentrations of <sup>228</sup>Ac and that of <sup>238</sup>U was determined from the average concentrations of the <sup>226</sup>Ra. The activity concentrations of <sup>238</sup>U-series (<sup>226</sup>Ra), <sup>232</sup>Th series (<sup>228</sup>Ac), as well as <sup>40</sup>K, expressed in Bq/Kg. The range of lowest (minimum), highest (maximum) and average values of the activity concentration of the natural radionuclides in each area are given in Table II. The activity concentrations of <sup>238</sup>U as estimated on the basis of <sup>226</sup>Ra activity concentrations. Activity concentrations of <sup>238</sup>U (<sup>226</sup>Ra) ranged from 0.51±0.07 to 9.32±0.32 Bq/Kg with an average (mean) value of 5.65±0.22 Bq/Kg.

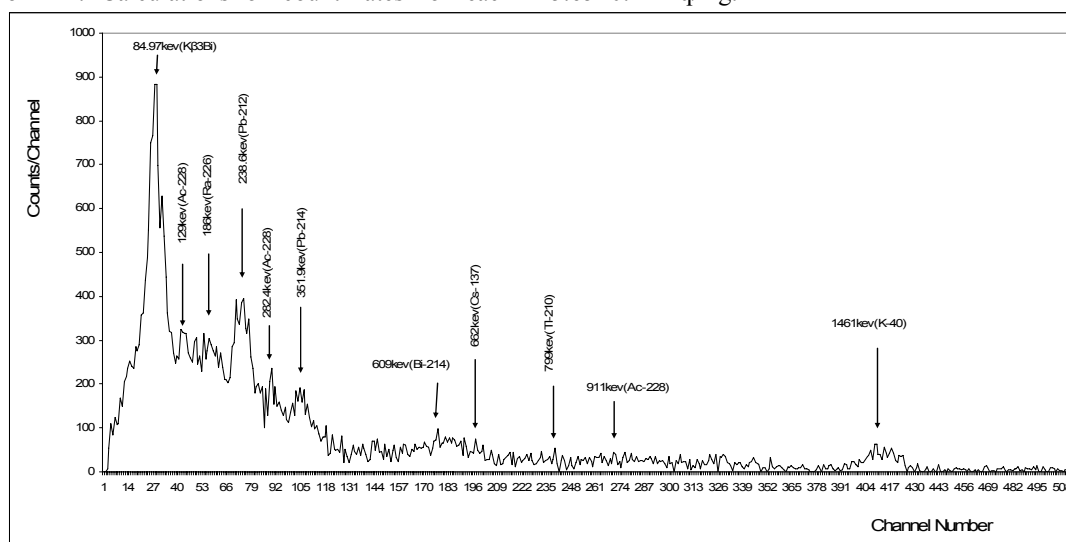


Fig. 4 Natural gamma-ray spectrum of sample (4) in the energy range of (84-1816) keV, taken by the NaI(Tl) detector.

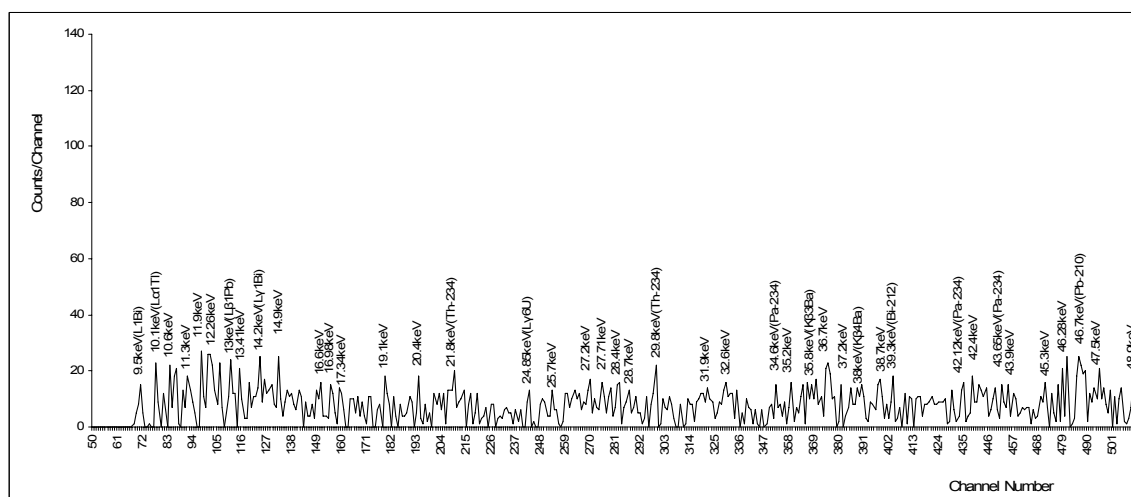


Fig. 5 Natural gamma-ray spectrum of sample (4) in the energy range of (9.5-50) keV, taken by the HPGe detector.

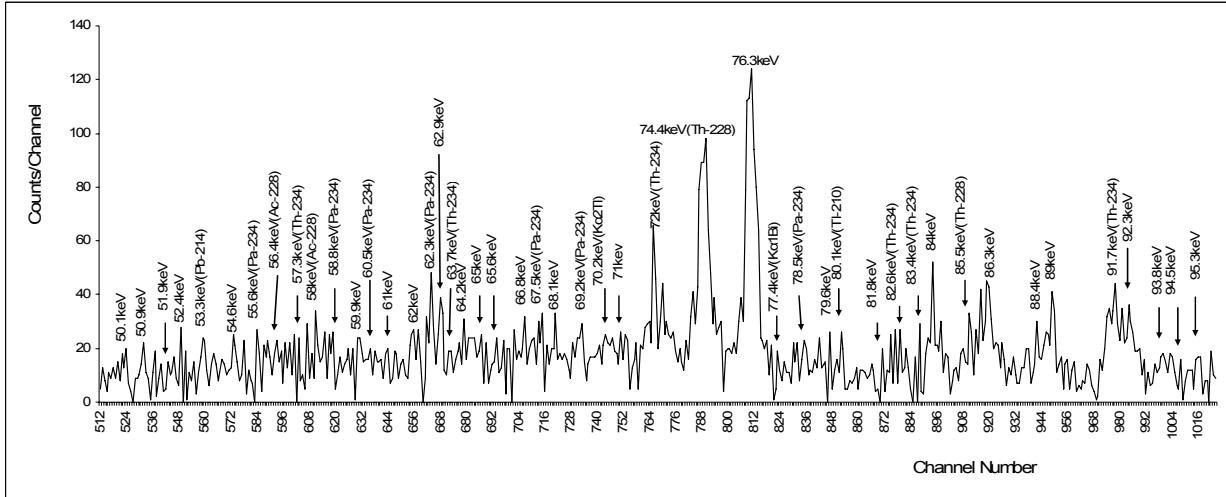


Fig. 6 Natural gamma-ray spectrum of sample (4) in the energy range of (50-100) keV, taken by the HPGe detector.

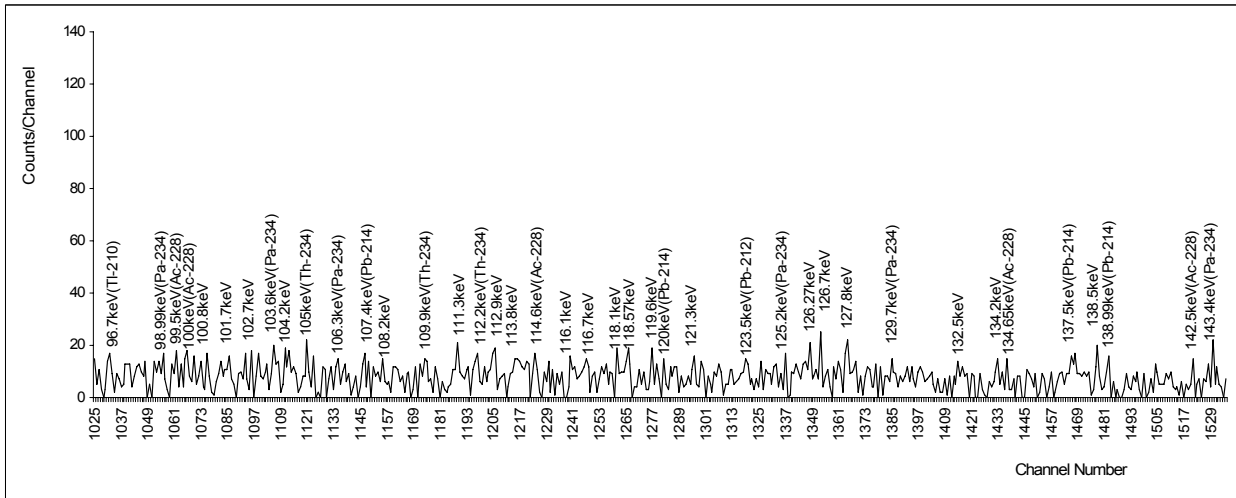


Fig. 7 Natural gamma-ray spectrum of sample (4) in the energy range of (100-145) keV, taken by the HPGe detector.

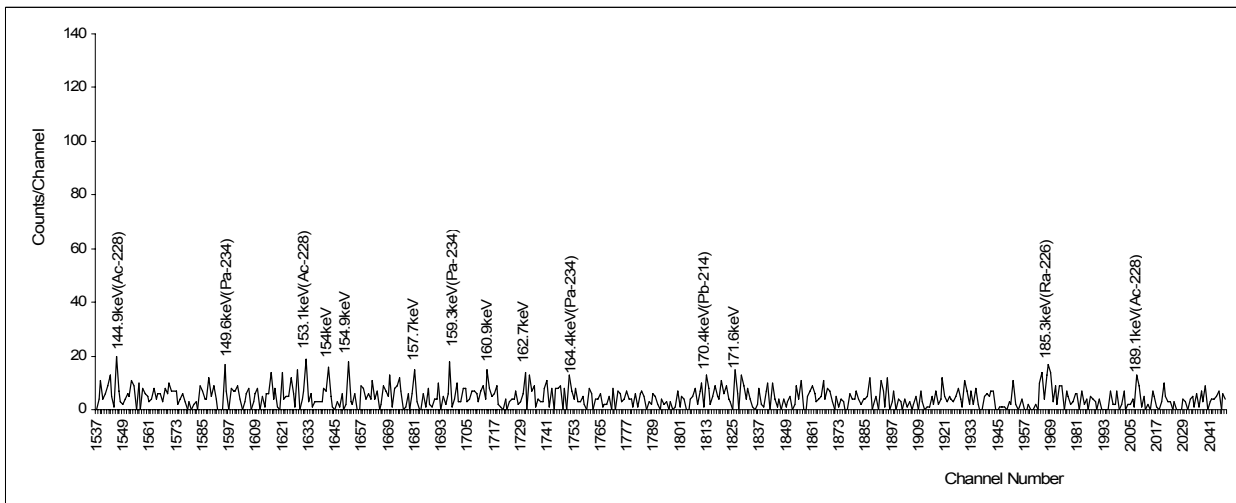


Fig. 8 Natural gamma-ray spectrum of sample (4) in the energy range of (145-186) keV, taken by the HPGe detector.

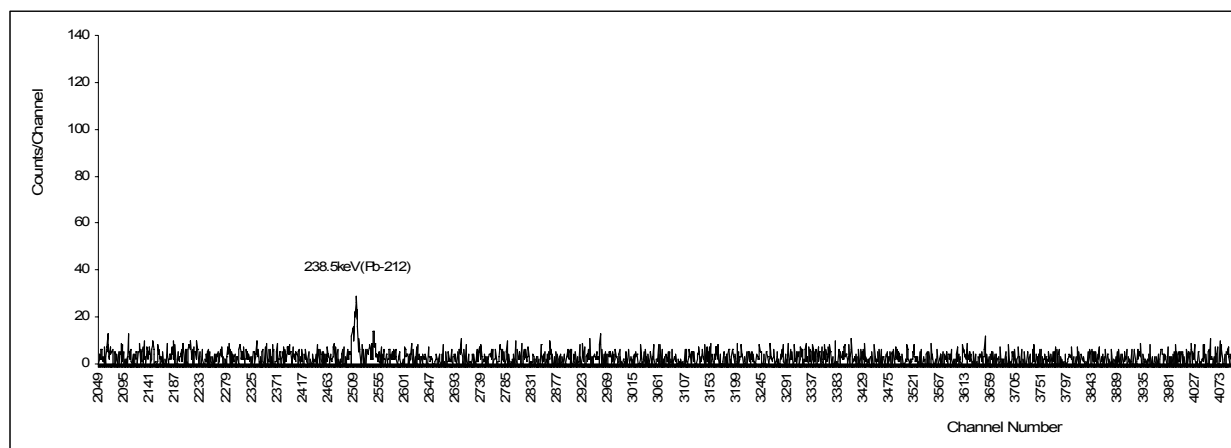


Fig. 9 Natural gamma-ray spectrum of sample (4) in the energy range of (186-400) keV, taken by the HPGe detector.

Also the activity concentrations of  $^{232}\text{Th}$  in investigated rocks were estimated on the basis of  $^{228}\text{Ac}$  activity concentration. The  $^{228}\text{Ac}$  ( $^{232}\text{Th}$ ) activity concentration was ranged from  $6.52 \pm 1.03$  to  $37 \pm 2.45$  Bq/Kg with an average value of  $21.4 \pm 1.78$  Bq/Kg.

Table III presents a comparison of the obtained activity concentrations with those calculated in other countries. This comparison is also illustrated in Fig. (12).

The values of concentration followed by contents of concentration in % for  $^{40}\text{K}$  and in ppm for  $^{232}\text{Th}$  and  $^{238}\text{U}$  are shown in Table IV. Fig.(13) shows the contents of each radionuclide. The higher values of activity concentrations of  $^{226}\text{Ra}$  (Bq/Kg),  $^{228}\text{Ac}$  (Bq/Kg) and  $^{40}\text{K}$  (Bq/Kg) are noted in sample 6 (Rubarok)  $9.32 \pm 0.32$ , sample 7 (Kanishilana)  $37 \pm 2.45$  and sample 4 (Kanishilana)  $358.46 \pm 11.18$  respectively, these two regions located in the middle and down the mountain, while the lower values are noted in samples 2

(Rubarok)  $0.51 \pm 0.07$ , sample 8 (Bardbizin)  $6.52 \pm 1.03$  and  $67 \pm 4.84$  respectively, these samples are from regions located in top of the mountain. To obtain uranium concentration content in these rock samples, the value of  $^{238}\text{U}$  concentrations in ppm were calculated using (1 ppm U = 12.25 Bq/Kg  $^{238}\text{U}$ ) [19], the concentration contents of  $^{238}\text{U}$  is ranged from 0.042 to 0.76 ppm with an average value of 0.45 ppm as shown in Table IV. The value of  $^{228}\text{Ac}$  ( $^{232}\text{Th}$ ) concentration in ppm was calculated using (1ppm Th = 4.10 Bq/Kg  $^{232}\text{Th}$ ) [19]. The concentration of  $^{228}\text{Ac}$  ( $^{232}\text{Th}$ ) is ranged from 1.46 to 9.02 ppm with an average value of 5.2 ppm as shown in Table IV. The value of  $^{40}\text{K}$  concentrations are ranged from  $67 \pm 4.84$  to  $358.46 \pm 11.18$  Bq/Kg with an average value of  $203.34 \pm 8.12$  Bq/Kg, Table II, and the concentration of content in percent (%) was calculated, Concentration content of  $^{40}\text{K}$  ranged from 0.2 to 1.12 % with an average value of 0.63 % as shown in Table IV.

TABLE II

ACTIVITY CONCENTRATIONS IN (BQ.KG<sup>-1</sup>) OF  $^{238}\text{U}$ ( $^{226}\text{Ra}$ ),  $^{232}\text{Th}$ ( $^{228}\text{Ac}$ ),  $^{137}\text{Cs}$  AND  $^{40}\text{K}$  IN BASALT IGNEOUS ROCKS WHICH ARE MEASURED BY THE NAI(TL) DETECTOR.

Sample Code	Activity Concentration (Bq/Kg)			
	Ra-226	Ac-228	Cs-137	K-40
S1	5.046±0.23	17.61±1.69	1.33±0.10	73.44±5.00
S2	0.51±0.07	12.23±1.41	1.15±0.10	219.6±8.80
S3	6.97±0.27	34.9±2.30	0.92±0.09	342.87±11
S4	7.5±0.20	29.52±2.19	3.39±0.17	358.46±11.2
S5	6.99±0.27	11.09±1.34	2.46±0.14	251.06±9.41
S6	9.32±0.32	22.34±1.90	3.82±0.18	198.30±8.22
S7	1.22±0.11	37±2.45	0.85±0.08	116±6.51
S8	7.68±0.29	6.52±1.03	2.56±0.15	67±4.84
Mean Value	5.65±0.22	21.4±1.78	2.05±0.12	203.34±8.12

TABLE III

COMPARISON OF MEAN ACTIVITY CONCENTRATION WITH OTHER WORKS

Country	Radionuclide		
	U-238(Ra-226)	Th-232(Ac-228)	K-40
Kurdistan, Iraq (2010)	5.65	21.4	203.34
Egypt (2008)	13.72	14.46	405.73
Poland (2006)	25.41	18.1	204.2
Kenya (2004)	18.66	18.7	401.7
Greece (2002)	29	3	361

### C. $^{137}\text{Cs}$ Activity Concentration

Activity concentration of  $^{137}\text{Cs}$  radionuclide is shown in Table II and illustrated in Figs. (10) and (11). This value ensures that there is low activity concentration of  $^{137}\text{Cs}$  in basalt igneous rocks. The highest and lowest values of activity concentrations to be noted in the sample 6 (Rubarok)  $3.82 \pm 0.18$  Bq/Kg and sample 7 (Kanishilana)  $0.85 \pm 0.08$  Bq/Kg respectively, these samples are located in the middle of



mountain and so the radioactive fallout was no high as it is noted. The observed average activity concentration of  $^{137}\text{Cs}$  has been compared with those of the other countries as presented in Table III, and illustrated in Fig. (12).

TABLE IV  
 $^{238}\text{U}$ ,  $^{232}\text{Th}$  AND  $^{40}\text{K}$  CONTENT IN SAMPLES WHICH ARE MEASURED BY NAI(TI) DETECTOR

Sample Code	Radionuclide Concentration		
	U(ppm)	Th(ppm)	K(%)
S1	0.41	4.29	0.22
S2	0.042	2.98	0.68
S3	0.56	8.51	1.07
S4	0.61	7.2	1.12
S5	0.57	2.77	0.78
S6	0.76	5.44	0.61
S7	0.09	9.02	0.36
S8	0.62	1.46	0.2
Mean Value	0.45	5.2	0.63

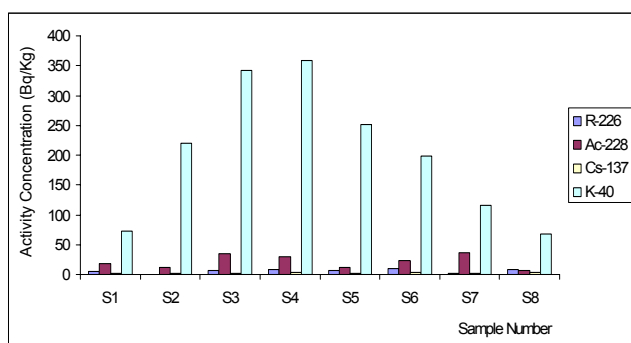


Fig. 10 Activity concentration in (Bq/Kg) of  $^{238}\text{U}$  ( $^{226}\text{Ra}$ ),  $^{232}\text{Th}$  ( $^{228}\text{Ac}$ ),  $^{137}\text{Cs}$  and  $^{40}\text{K}$ .

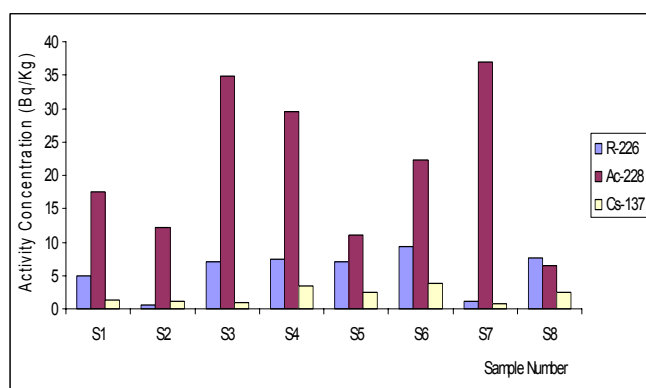


Fig. 11 Activity concentration in (Bq/Kg) of  $^{238}\text{U}$  ( $^{226}\text{Ra}$ ),  $^{232}\text{Th}$  ( $^{228}\text{Ac}$ ) and  $^{137}\text{Cs}$ .

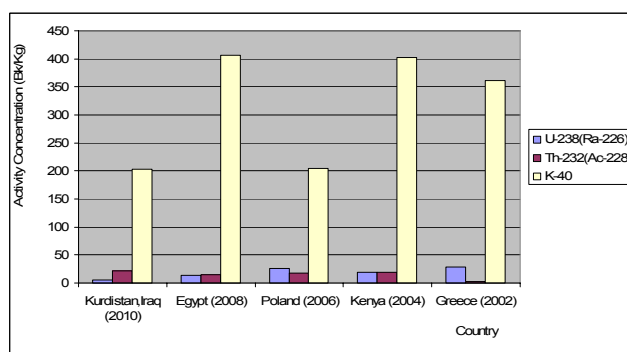


Fig. 12 Comparison of the resulted activity concentration with those of other countries.

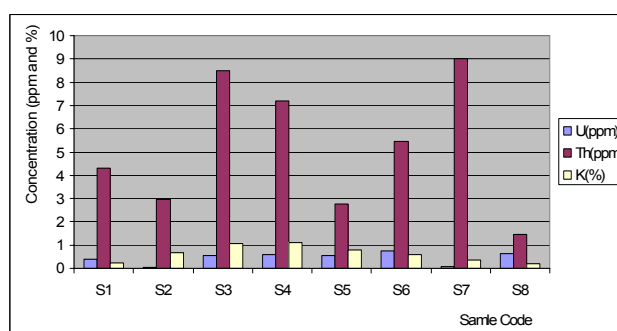


Fig. 13 The  $^{238}\text{U}$ ,  $^{232}\text{Th}$  and  $^{40}\text{K}$  Content.

#### D. Radiation hazard indices

It is important to assess the gamma radiation hazards to human associated with the used samples for buildings; these were done by calculating the different radiation hazard indices. The radium equivalent activities  $Ra_{eq}$  (Bq/Kg) of samples under investigation were calculated on the basis of equation (3) and shown in Table V, the resulted values ranged from 22.16 to 77.31 Bq/Kg with an average value of 44.8 Bq/Kg, this value is below the internationally accepted value 370 Bq/Kg [12].

Along the study area the absorbed dose rate  $D$  ( $\text{nGyh}^{-1}$ ) which expressed in equation (4) ranged from 10.39 to 39.19 ( $\text{nGyh}^{-1}$ ) with an average value of 24.81  $\text{nGyh}^{-1}$  these calculated values were lower than the estimate of average global terrestrial radiation of 55 ( $\text{nGyh}^{-1}$ ) [12]. Indoor and outdoor annual effective dose rate  $E_{ied}$  ( $\text{mSvy}^{-1}$ ) and  $E_{oed}$  ( $\text{mSvy}^{-1}$ ) from these basalt rock samples are determined from equations (7) and (8) and ranged from 0.05 to 0.19  $\text{mSvy}^{-1}$  with an average value of 0.11  $\text{mSvy}^{-1}$  and from 0.012 to 0.048  $\text{mSvy}^{-1}$  with an average value of 0.03  $\text{mSvy}^{-1}$  respectively. The External hazard index and internal hazard index are calculated using equations (5) and (6) the External hazard index,  $H_{ex}$  for the basalt rock samples studied in this work ranged from 0.059 to 0.22 with an average value of 0.138, the computed internal hazard index  $H_{in}$  values vary from 0.08 to 0.24 with an average value of 0.154. The values of  $H_{ex}$  and  $H_{in}$

TABLE V

RADIUM EQUIVALENT ACTIVITY  $Ra_{eq}$  (BQ.KG<sup>-1</sup>), ABSORBED GAMMA DOSE RATE D (NGYH<sup>-1</sup>), ANNUAL INDOOR EFFECTIVE DOSE RATE (MSVY<sup>-1</sup>) AND ANNUAL OUTDOOR EFFECTIVE DOSE RATE (MSVY<sup>-1</sup>) WITHIN THE STUDIED SAMPLES

Sample Code	Radiation Hazard Indices			
	$Ra_{eq}$ (Bq.Kg <sup>-1</sup> )	D (nGyh <sup>-1</sup> )	$E_{ied}$ (msvy <sup>-1</sup> )	$E_{oed}$ (msvy <sup>-1</sup> )
S1	35.88	16.33	0.08	0.020
S2	34.91	16.99	0.083	0.020
S3	26.4	39.19	0.19	0.048
S4	77.31	36.74	0.18	0.045
S5	42.18	23.91	0.11	0.029
S6	56.53	26.44	0.12	0.032
S7	63.06	28.49	0.13	0.034
S8	22.16	10.39	0.05	0.012
Mean Value	44.8	24.81	0.11	0.03

TABLE VI

EXTERNAL HAZARD INDEX  $H_{ex}$  (BQ.KG<sup>-1</sup>), INTERNAL HAZARD INDEX  $H_{in}$ , REPRESENTATIVE LEVEL INDEX  $I_{\gamma r}$  WITHIN THE STUDIED SAMPLES

Sample Code	Radiation Hazard Indices		
	$H_{ex}$	$H_{in}$	$I_{\gamma r}$
S1	0.096	0.11	0.258
S2	0.094	0.095	0.272
S3	0.22	0.24	0.624
S4	0.20	0.229	0.584
S5	0.113	0.132	0.324
S6	0.152	0.177	0.417
S7	0.170	0.173	0.455
S8	0.059	0.080	0.161
Mean Value	0.138	0.154	0.386

of all samples studied in this work were less than unity [11], which are acceptable global values. The value of radiation hazard index called the representative level index  $I_{\gamma r}$  which expressed in equation (9) must be less than unity for the radiation hazard to be negligible, the value of representative level index for the studied samples in this work ranging from 0.161 to 0.624 with an average value of 0.386. The  $I_{\gamma r}$  values are below the internationally accepted value 1 [12]. The highest and lowest values of  $Ra_{eq}$  (Bq/Kg) are noted in sample 4 (Kanishilana) 77.31 and sample 8 (Bardbizin) 22.16, respectively, these two location of samples located to the top and the down of the mountain. The highest values of D (nGyh<sup>-1</sup>),  $E_{ied}$  (mSvy<sup>-1</sup>) and  $E_{oed}$  (mSvy<sup>-1</sup>) are noted in the sample 3 (Bardbizin) 39.19, 0.19 and 0.048 respectively, which is located to the middle of the mountain and the lowest values was in sample 8 (Bardbizin) 10.39, 0.05 and 0.012 respectively, top of the mountain. The highest values of  $H_{ex}$ ,

$H_{in}$  and  $I_{\gamma r}$  are noted in sample 3 (Bardbizin) 0.22, 0.24 and 0.624 respectively, which is located in the middle of the mountain, while the lowest values is noted in sample 8 (Bardbizin) 0.059, 0.08 and 0.161, respectively, at top of the mountain.

#### IV. CONCLUSIONS

The results of gamma-ray measurements presented in this work give current information about natural and man-made radioactivity of basalt igneous rock samples collected from the Sidakan zone of the Kurdistan region-Iraq. The results reveal the existence of U and Th natural series, K-40, and <sup>137</sup>Cs radionuclide's in a variety percentages depending on the location of samples within the mountain, approving the fact that for the lower regions large radionuclide's accumulation occurs which yield higher concentrations and vice versa. The average values of <sup>226</sup>Ra, <sup>228</sup>Ac, <sup>40</sup>K and <sup>137</sup>Cs activity, radium equivalent activity  $Ra_{eq}$ , gamma dose rate D, indoor and outdoor annual effective dose rate  $E_{ied}$  and  $E_{oed}$ , external hazard index and internal hazard index  $H_{ex}$  and  $H_{in}$ , and representative level index  $I_{\gamma r}$  were all found to be lower than the worldwide average values.

#### ACKNOWLEDGMENT

Authors would like to acknowledge the Geology Department, Science College, Salahaddin University especially Dr. Ahmed Akrawi and Mr. Awara Amin whom helps us in samples collection and preparation.

#### REFERENCES

- [1] Gwww.umich.edu/~radinfo/introduction/natural.html taken on 1/11/2002.
- [2] Alias A. et al., The Malaysian Journal of Analytical Sciences, Vol. 12, No. 1, (2008).
- [3] Mahur A. K. et al., Indian journal of Pure & Applied Physics, Vol. 48, July (2010), pp. 486-492.
- [4] Yang Ya-Xin. et al., Applied Radiation and Isotopes, 63 (2005) 255-259.
- [5] Jasaitis D., and Girgzdys A., Journal of Environmental Engineering and Landscape Management, Vol. XV, No. 1, (2007), pp. 313-7.
- [6] Ward G.M., Johnson J.E., and Wilson D.W., Colorado Agricultural Experiment Station, Vol. 81, No.7, (1966).
- [7] Erbil Governorate Profile, Inter-Agency Information and Analysis Unit (IAU), July (2009).
- [8] Germanium Detectors, User's Manual, Canberra Industries, Inc., (1989).
- [9] Hassan H. I., and Mheemeed A. Kh., Damascus University Journal for Basic Sciences Vol. 24, No. 2, (2008).
- [10] Sujo L.C. et al., Journal of Environmental Radioactivity 77 (2004) 205-219.
- [11] Diab H. M. et al., Journal of Nuclear and Radiation Physics, Vol. 3, No. 1, (2008), pp. 53-62.
- [12] Harb S. et al., Proceedings of the 3rd Environmental Physics Conference, 19-23 Feb. (2008), Aswan, Egypt.
- [13] Bé M. -M. et al., Table of Radionuclides, Vol. 2-A=151 to 242, (2004).
- [14] Bé M. -M. et al., Table of Radionuclides, Vol. 4-A=133 to 252, (2008).
- [15] [http://www.nucleide.org/DDEP\\_WG/Nuclides/Cs-137\\_tables.pdf](http://www.nucleide.org/DDEP_WG/Nuclides/Cs-137_tables.pdf), 2/2007.
- [16] [http://www.nucleide.org/DDEP\\_WG/Nuclides/K-40\\_tables.pdf](http://www.nucleide.org/DDEP_WG/Nuclides/K-40_tables.pdf), 3/6/2009.
- [17] Auble R. L. et al., Nuclear Data Sheets, Vol. 21, No. 4, (1977).
- [18] Tuli J. K., Nuclear Data Sheets, Vol. 49, No. 1, (1986).
- [19] Maphoto K. P., M. Sc. Thesis, University of the Western Cape, South Africa, (2004).